Applied Catalysis B: Environmental 108–109 (2011) 152–160

Contents lists available at SciVerse ScienceDirect

Applied Catalysis B: Environmental

journal homepage: www.elsevier.com/locate/apcatb

# Effect of preparation of Pd and Pd–Pt catalysts from acid leached silica–alumina on their activity in HDS of thiophene and benzothiophene

Zdeněk Vít[a,*], Hana Kmentová[a], Luděk Kaluža[a], Daniela Gulková[a], Marta Boaro[b]

[a] Institute of Chemical Process Fundamentals of the ASCR, v.v.i., Rozvojová 135, 165 02 Prague, Czech Republic
[b] Department of Chemistry, Physics and Environment, University of Udine, I-33100 Udine, Italy

ARTICLE INFO

*Article history:*
Received 6 May 2011
Received in revised form 3 August 2011
Accepted 18 August 2011
Available online 25 August 2011

*Keywords:*
Hydrodesulfurization
Silica–alumina
Acid leaching
Pd catalyst
Pd–Pt catalyst

ABSTRACT

Mesoporous silica–alumina (MSA) modified by post-synthesis acid leaching was studied as a support for Pd and Pd–Pt catalysts. Activity of catalysts was evaluated in hydrodesulfurization (HDS) of model compounds (thiophene and benzothiophene). The leaching decreased the $Al_2O_3$ content of MSA from 52 to 9 wt.%. This treatment mainly removed the non-acidic extra-framework $Al_{oct}$ species, exposed the Brønsted acidic sites and increased the BET surface area by 50%. The higher acidity and surface area improved the activities of Pd catalysts in HDS of thiophene and benzothiophene. $Pd(OAc)_2$ deposited on the leached MSA gave the best monometallic Pd catalyst. Two bimetallic Pd–Pt catalysts were prepared by co-impregnation of the leached MSA with $Pd(OAc)_2 + Pt(NH_3)_4(OH)_2$ and $Pd(OAc)_2 + H_2PtCl_6$. The bimetallic catalyst prepared from $Pt(NH_3)_4(OH)_2$ showed significant promotional effect and exhibited the highest activity in HDS of thiophene and benzothiophene.



## 1. Introduction

Increasing demands for more efficient hydrotreatment of oil fractions has stimulated research of non-conventional catalysts based on novel active phases and supports. Noble metals of the 2nd and 3rd rows show promising activities in sulfur and nitrogen removal and thus some of them had often been studied as an alternative to traditional alumina-supported CoMo and NiMo sulfides. In addition, these metals usually show excellent hydrogenation (HYD) activity, which should facilitate removal of the most refractory sulfur compounds. Alumina- and titania-supported Pd and Pt catalysts proved to be highly active in naphthalene hydrogenation in the presence of benzothiophene [1]. Pd/alumina catalyst was superior in HYD of phenanthrene and only moderate in hydrodesulfurization (HDS) of dibenzothiophene, while combination of both metals led to high HYD and HDS activities [2]. For the purpose of HDS or HYD, Pd, Pt and bimetallic Pd–Pt active phases have often been deposited on acidic supports like zeolites. This is because Brønsted acidic sites are supposed to directly participate in the reaction and facilitate HDS [3]. Moreover, it was suggested that the acidity of these supports increases the electron-deficient character of deposited metal particles, which brings about their higher sulfur tolerance and consequently the better activity [4,5]. Amorphous silica–alumina (ASA) is frequently used support, along with zeolites. In contrast to the latter, the acidity of ASA is lower and the pore size larger, which diminishes undesirable cracking and makes the diffusion of bulky molecules easier. The ASA supported Pd and Pd–Pt catalysts have recently been studied in HYD of model compounds in the presence of sulfur in the feed [6], HYD of gas oil [7] and also in deep HDS of dibenzothiophene and different substituted dibenzothiophenes [8–10]. Discovery of new mesoporous solids like SBA-15 and MCM-41 initiated studies on their role as the supports for Pd catalysts in HDS of different model compounds. Generally low acidity of these siliceous supports has been increased by post-synthesis addition of aluminum [11,12] or by their mixing with HY zeolite [13], which positively affected the HDS activity of prepared Pd catalysts. The properties of supports such as zeolites and MCM-41 were also modified by leaching with different agents, including diluted acids. Treatment of Y zeolite with nitric acid removed part of the polymeric extra-framework aluminum species responsible for blocking of the pores and increased its crystallinity [14]. In the case of mesoporous MCM-41, this procedure increased the surface area, generated strong acidity and led to the higher activity of NiMo/MCM-41catalyst in HDS of dibenzothiophene [15].

Recently, we have synthesized a mesoporous silica–alumina (MSA) containing 50 wt.% $Al_2O_3$ by cogelification from simple inorganic salts [16]. This material was at first employed as a support of Mo sulfide catalysts promoted by Pt in HDS of thiophene and hydrodenitrogenation of pyridine [17,18]. A relatively high $Al_2O_3$ content was necessary to achieve a good dispersion of the deposited $MoS_2$ phase. Later, this MSA was considered as a support of the reduced Pt catalysts in HDS. The composition of MSA was thus modified by

* Corresponding author. Tel.: +420 220 390 284; fax: +420 220 920 661.
*E-mail address:* vit@icpf.cas.cz (Z. Vít).

0926-3373/$ – see front matter © 2011 Elsevier B.V. All rights reserved.
doi:10.1016/j.apcatb.2011.08.022

post-synthesis acid treatment with diluted nitric acid in attempt to increase its acidity [19]. The content of $Al_2O_3$ was progressively diminished from 50 to 11 wt.%. The resulting material preserved a good mechanical strength, showed larger surface area and stronger Brønsted acidity than the original one. This was ascribed to the removal of surplus non-acidic $Al_2O_3$ phase, hindering the accessibility of the strong acid sites of the silica–alumina matrix. The Pt catalysts prepared from so modified supports showed improved HDS activities. Some samples were substantially more active in HDS of thiophene and benzothiophene than the Pt catalyst prepared from HY zeolite and an industrial $CoMo/Al_2O_3$ sulfide catalyst.

The aim of this work was to verify if leaching of MSA improves HDS activities of Pd and bimetallic Pd–Pt catalysts similarly as it was previously found for the Pt catalysts and also to find proper conditions for the deposition of these active phases. For this purpose, a new batch of MSA support was synthesized and nitric acid was again chosen as a leaching agent. Three Pd precursors were used for preparation of monometallic Pd catalysts from both as-synthesized and modified supports. Bimetallic Pd–Pt catalysts were prepared from the best Pd precursor and the leached support by co-impregnation with two Pt precursors. The activities of noble metal catalysts were compared with that of sulfided industrial $CoMo/Al_2O_3$ in HDS of thiophene and benzothiophene.

## 2. Experimental

### 2.1. Preparation of supports and catalysts

MSA was synthesized from aqueous solutions of sodium metasilicate and aluminum nitrate by the procedure described in detail elsewhere [16]. The support was finally calcined at 500 °C for 6 h, crushed and sieved to 0.16–0.315 mm particles. The bulk composition corresponded to 52 wt.% $Al_2O_3$ and 48 wt.% $SiO_2$. The sample with the reduced $Al_2O_3$ content was prepared by leaching of this basic support with 1 N nitric acid in a rotary evaporator at 75 °C for 2 h. The product was washed with distilled water, dried and calcined at 400 °C for 2 h. It contained 9 wt.% $Al_2O_3$ and 91 wt.% $SiO_2$. Both supports are referred to as MSA52 and MSA9, where number gives the $Al_2O_3$ content in wt.%.

Monometallic Pd catalysts were prepared by impregnation of both supports with aqueous solutions of $Pd(NH_3)_4Cl_2{\cdot}H_2O$ and $PdCl_2$ and acetone solution of Pd acetate ($Pd(OAc)_2$) at room temperature (r.t.) for 1 h. In the case of $PdCl_2$ and $Pd(NH_3)_4Cl_2{\cdot}H_2O$, pH of the solutions was adjusted with HCl and $NH_4OH$ to 3 and 10, respectively. The Pt catalysts were prepared by impregnation of MSA9 with aqueous solutions of $Pt(NH_3)_4(OH)_2$ and $H_2PtCl_6$. Two bimetallic Pd–Pt catalysts were prepared by co-impregnation of MSA9 with acetone–water solutions of $Pd(OAc)_2 + Pt(NH_3)_4(OH)_2$ and $Pd(OAc)_2 + H_2PtCl_6$. The amounts of the precursors were chosen to approach the Pd loading close to 1 wt.% and the atomic Pd:Pt ratio near to 4. Similar Pd:Pt ratio and co-impregnation procedure usually gave the most active Pd–Pt catalysts in other studies [4,7,8]. The volume of the solutions was usually 5 ml per g of support. The slurries were evaporated to dryness in a rotary evaporator at 60 °C under vacuum. The dried catalyst precursors were reduced in $H_2$ at 400 °C (ramp 4 °C/min and dwell 1 h at 400 °C) and stored. The temperature 400 °C was chosen to completely reduce the noble metal salts and release ammonia from acidic sites of the supports. The monometallic catalysts were marked by symbols like 0.92PdA-9, giving sequentially the metal content in wt.%, metal precursor and the content of $Al_2O_3$ in the support. The symbols PdA, PdC, PdN, PtO and PtC stand for $Pd(OAc)_2$, $PdCl_2$, $Pd(NH_3)_4Cl_2{\cdot}H_2O$, $Pt(NH_3)_4(OH)_2$ and $H_2PtCl_6$, respectively. The bimetallic catalysts were denoted as Pd–PtO-9 and Pd–PtC-9. The $CoMo/Al_2O_3$ catalyst (Shell 344, 2.4 wt.% Co, 9.2 wt.% Mo) was used as a typical HDS catalyst for comparative purpose as in our previous study [19]. It was sulfided with 10% $H_2S$ in $H_2$ at 400 °C for 2 h before reactions.

### 2.2. Characterization of supports and catalysts

The chemical composition was determined by inductively coupled plasma-atomic absorption spectroscopy (ICP/AAS). BET surface areas and pore-size distributions of the samples degassed at 400 °C were determined by $N_2$ adsorption with an ASAP2010 M instrument (Micromeritics). The $^{27}Al$ MAS NMR spectra were recorded at 130.33 MHz on a Bruker Avance 500 WB/US NMR spectrometer (Germany) using a magic angle spinning (MAS) frequency of 11 kHz. The finely ground samples (80 mg) were placed in 4 mm $ZrO_2$ rotor. The pulse length was 0.8 μs and the repetition delay of 2 s. $^{27}Al$ NMR chemical shifts were reported relative to $Al(NO_3)_2{\cdot}6H_2O$ (0.0 ppm). The spectra were deconvoluted by the DmFit program in order to obtain relative amounts of different Al species. The point of zero charge (PZC) values of the supports were determined in aqueous suspensions after 1 h equilibration at r.t. on a WTW pH meter with Hamilton Slimtrode cell.

Pd and Pt dispersions were determined by CO sorption on a commercial Autochem 2920 instrument (Micromeritics). A total of 50 mg of catalyst was reduced by 5% $H_2$ in Ar at 400 °C, purged by He at 400 °C for 1 h and cooled to 0 °C in He. The catalyst was then titrated by pulses of 5% CO in He. The CO:Pd = 1:2 stoichiometry was adopted for calculation of Pd dispersion [20–23]. In the case of Pt catalysts, the CO:Pt = 1:1 stoichiometry was used [24]. The overall dispersion of the bimetallic Pd–Pt catalysts was calculated by using the above stoichiometries and taking into account molar fractions of both metals in the catalysts. X-ray diffraction (XRD) of the Pd catalyst was carried out on a Philips PW3040/60 X'pert PRO instrument equipped with Ni-filtered Cu Kα radiation and operated at 40 kV/40 mA. Diffraction profiles for Pd crystal size were collected in the 34–46° range of $2\theta$, with a step width of 0.01 and a counting time of 80 s/step.

The temperature programmed reduction (TPR) of the dried catalyst precursors was performed in a conventional apparatus by monitoring $H_2$ consumption with the thermal conductivity detector (TCD). The sample (200 mg) in a quartz U tube was heated to 900 °C by ramp 5 °C/min in the mixture of 5 vol.% $H_2$ in Ar (35 ml/min). A column with molecular sieve Linde 13X was placed before TCD in order to trap the evolved water and ammonia. The temperature programmed desorption (TPD) of $H_2$ released from the reduced and $H_2$-saturated catalysts was carried out in the same apparatus by a procedure similar to that proposed by Pinna and coworkers [20]. The catalysts were in situ re-reduced by $H_2$ at 400 °C/0.5 h, cooled to room temperature in $H_2$ for 0.5 h and purged by mixture of 5% $H_2$ in Ar (35 ml/min) for 0.5 h. Then the temperature was raised to 140 °C (ramp 15 °C/min) in a flow of $H_2$/Ar mixture and the $H_2$ desorbed from the catalyst was monitored by TCD. After each TPD run, TCD was calibrated by 25 μl $H_2$ pulses generated by use of a 6-port sampling valve. The amounts of desorbed $H_2$ and H/Pd ratios were calculated from the peak areas, catalyst weight and Pd loading. Deconvolution of the TPD pattern into individual peaks was carried out by a PFM program.

### 2.3. Catalytic tests

#### 2.3.1. Cyclohexene isomerization and cumene cracking

The acidity of the supports was characterized by their activities in cyclohexene (CH) isomerization and cumene (CU) cracking, both catalysed by Brønsted acidic sites [25]. The conversions of both compounds were taken as simple indices of the support acidities, similarly as in our preceding work [19]. The activity was evaluated in a flow microreactor with the fixed catalyst bed at 240 °C and 0.5 MPa [26]. The CH steady state conversions into

**Table 1**
Composition, properties and activities of supports in cyclohexene and cumene conversions.

| Support | $Al_2O_3$ (wt.%) | Na (wt.%) | $S_{BET}$ ($m^2/g$) | $V_p$ ($cm^3/g$) | $Al_{tet}$ (%) | $Al_{pent}$ (%) | $Al_{oct}$ (%) | PZC | $x_{CH}^{240}$ | $x_{CU}^{400}$ |
|---|---|---|---|---|---|---|---|---|---|---|
| MSA52 | 52 | 0.33 | 429 | 0.41 | 22 | 3 | 75 | 6.0 | 0.58 | 0.69 |
| MSA9 | 9 | 0.01 | 643 | 0.65 | 53 | 0 | 47 | 3.8 | 0.82 | 0.77 |

1-methylcyclopentene (1-MCPE) were evaluated during 4 h on stream. A gas chromatograph (GC) Agilent 4890D operated with FID detector and 30 m capillary DB-5 column (0.25 mm) at 50 °C. The cracking activity was tested at 370 °C and 0.5 MPa in the same apparatus. The procedure was essentially the same as for the isomerization. The conversions into benzene and propylene were evaluated during 3–5 h on stream. The analyses were performed on the same column at 115 °C.

#### 2.3.2. Thiophene HDS

The activity of the catalysts in HDS of thiophene (TH) was evaluated in another flow microreactor with fixed bed of catalyst at 280 °C and 2 MPa, as described in detail elsewhere [19]. The feed, generated by passing $H_2$ through a pressure saturator filled with TH, contained 240 ppm of TH in $H_2$ (150 ml/min). The flow rate of the feed $F_{TH}$ was constant ($9.7 \times 10^{-5}$ $mol_{TH}/h$). The catalyst amount W varied between 6 and 21 mg. The catalysts were at first in situ re-activated by $H_2$ at 400 °C/1 h. Then the reaction was carried out at 280 °C during 4–6 h. The steady state was achieved within 2–3 h on stream, and then the conversions were calculated from several analyses. The samples of the feed and the reaction mixture were taken automatically by a 6-port sampling valve. The on-line analyses were carried out on a GC HP 5890 equipped with FID detector and 3.5 m packed column (Carbopack B 60/80 4% Carbowax 20 M) at 125 °C. The products were $C_4$ hydrocarbons, $H_2S$ and tetrahydrothiophene (THT). The activities were expressed both by overall TH conversions, $x_{TH}$, conversions in THT, $x_{THT}$, conversions in $C_4$ hydrocarbons, $x_{C4}$ and by the pseudo-first-order rate constants $k_{TH}$, calculated according to $k_{TH} = -(F_{TH}/W)\ \ln(1 - x_{TH})$. The percentage of deactivation (Deact.) was expressed as $100(x_{TH}^o - x_{TH})/x_{TH}^o$, where $x_{TH}^o$ is initial TH conversion. The $k_{TH}^o$ symbol stands for the initial activity.

#### 2.3.3. Benzothiophene HDS

The activity of the catalysts in HDS of benzothiophene (BT) was evaluated in the gas phase in a flow reactor with fixed bed of catalyst at 330 °C and 1.6 MPa [19,27]. The liquid feed was fed by a Waters 510 HPLC pump into evaporator section connected to the reactor and separation system. The feed rate $F_{BT}$ was $7.7 \times 10^{-3}$ $mol_{BT}/h$ and the constant feed composition was 16 kPa, 200 kPa and 1384 kPa of BT, decane and hydrogen, respectively. The catalyst ($W$ = 40 or 200 mg) was diluted with α-$Al_2O_3$ (Alfa Aesar) to obtain a 30 mm bed and before tests it was in situ re-activated by $H_2$ at 400 °C/1 h. The mixture of products was condensed in a cooler (Lauda RE 205) at −5 °C and the condensate was periodically drained off by a fine needle valve. The liquid samples were taken after their sufficient amount had been collected, usually in 1 h interval, and then analysed on a GC HP 6890 with a 30 m capillary HP-5 column (0.53 mm) using a temperature program between 130 and 180 °C. The products were ethylbenzene (EB), $H_2S$ and dihydrobenzothiophene (DHBT). Only minor activity decay was found between 1, 2 and 3 h of run, thus only data after 3 h on stream are given. The activities were expressed both by overall BT conversions $x_{BT}$, conversions to DHBT, $x_{DHBT}$, conversions to EB, $x_{EB}$ and by the rate constants $k_{BT}$, calculated analogously as those for TH. The magnitude of the synergetic effect (SE) in BT and TH reactions was expressed by the ratio of the rate constants over the bimetallic Pd–Pt catalyst and the sum of the rate constants over Pd and Pt catalysts as $SE = k_{Pd-Pt}/(k_{Pd} + k_{Pt})$.

## 3. Results and discussion

### 3.1. Properties of supports

Table 1 summarizes the properties of the original and modified MSA supports. The overall content of $Al_2O_3$ was diminished by leaching from 52 to 9 wt.%, which corresponds to about 80% extraction of the originally present $Al_2O_3$ phase. This process was also accompanied by parallel extraction of the residual sodium. This change of composition led to decrease of the PZC value of the support from 6.0 to 3.8. Fig. 1 shows the nitrogen adsorption isotherms of both supports. The isotherms were similar but that for the leached support showed smaller additional increment of the amount of adsorbed nitrogen above $p/p_o = 0.9$, suggesting the presence of larger pores. At the same time, the BET surface area and total pore volume $V_p$ of MSA9 sample increased by about 50%, compared to the values for MSA52 (Table 1). Nitrogen adsorption on both supports showed the presence of the pores of diameters between 2 and 10 nm. In addition, mercury porosimetry on MSA9 revealed also larger pores with diameters 30–200 nm. Their volume was 0.15 $cm^3/g$, i.e. about 23% of the total pore volume $V_p$ determined by nitrogen adsorption. This documents that the extraction of the major part of $Al_2O_3$ from MSA52 did not lead to any observable damage of the structure, but rather to its improvement in the sense of the higher surface area and total pore volume. However, too extensive leaching generated also a minor fraction of macropores.

The $^{27}Al$ MAS NMR spectra of both supports are shown in Fig. 2. The peak maxima for different Al species are located at about 7, 33 and 56 ppm. The signals at 7 and 56 ppm correspond to aluminum in octahedral ($Al_{oct}$) and tetrahedral ($Al_{tet}$) coordination, respectively, while the signal at 33 ppm is usually ascribed to the pentacoordinated aluminum ($Al_{pent}$) [28,29]. MSA52 contains the majority of aluminum in the octahedral form (Table 1). This is common for condensed non-acidic aluminum hydroxide- and oxyhydroxide-like

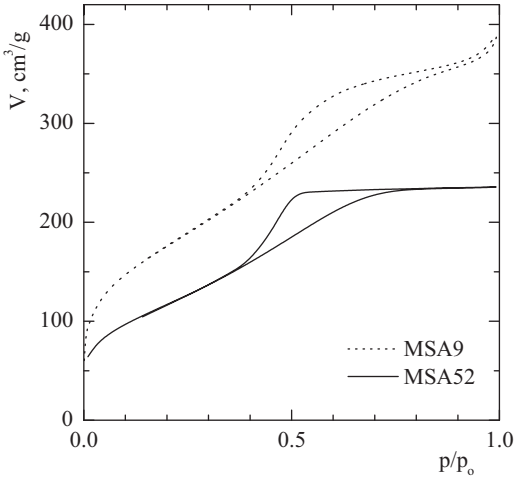


**Fig. 1.** Nitrogen adsorption isotherms of MSA9 and MSA52 supports.

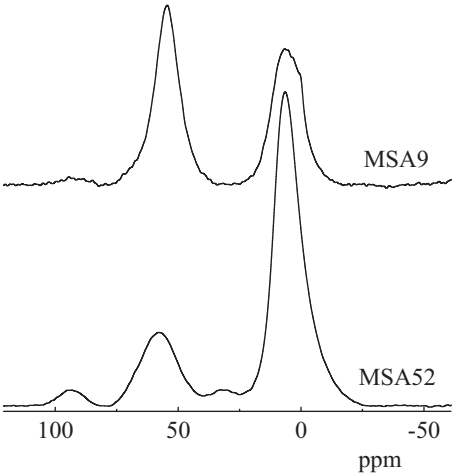


**Fig. 2.** $^{27}$AL MAS NMR spectra of MSA9 and MSA52.

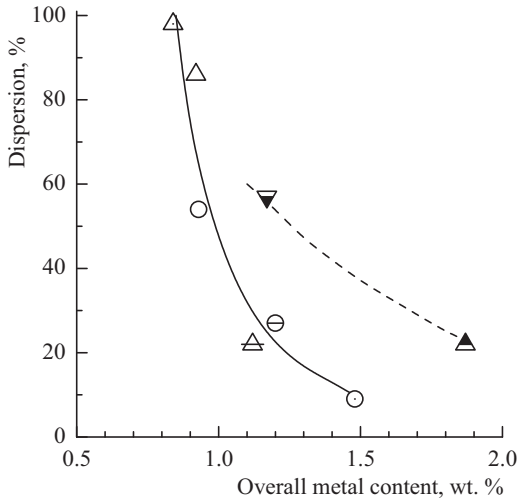


**Fig. 3.** Dispersion as a function of metal loading. 0.93PdA-52 (◯), 1.48PdC-52 (⊙), 1.20PdN-52 (⊖), 0.92PdA-9 (△), 0.84PdC-9 (△), 1.12PdN-9 (△), Pd–PtO-9 (▼); Pd–PtC-9 (▲).

structures [29]. Acid leaching eliminated mostly this form of extra-framework aluminum, along with total removal of $Al_{pent}$, located in the interface between silica–alumina phase and segregated $Al_2O_3$ domains. The bulk composition was thus greatly enriched by $Al_{tet}$ species, which become dominant in MSA9. As shown in Table 1, MSA9 was more active than MSA52 in both CH isomerization and CU cracking, confirming the increase of Brønsted acidity. This is in harmony with the idea that $Al_{tet}$ are associated with strongly acidic hydroxyls of silica–alumina [28]. Thus, the leaching of MSA52 in the present work had again similar cleaning effect as that observed earlier on zeolites [14], MCM-41 [15] and previously on MSA50 [19].

### 3.2. Properties of catalysts

The composition, CO uptake, metal dispersion and main textural properties of the reduced catalysts are given in Table 2. The majority of Pd catalysts contained around 1 wt.% Pd and two Pt catalysts around 0.5 wt.% Pt. In the case of bimetallic Pd–Pt samples, we attempted to obtain the composition close to atomic ratio Pd:Pt = 4, which was easier to achieve in the sample Pd–PtO-9 (Pd:Pt = 3.7). The overall metal loading was rather low and thus the BET surface areas and $V_p$ values of the catalysts remained relatively high, only slightly below the values for the parent supports.

The chemisorption stoichiometry CO:Pd = 1:2 was taken in this work for calculating Pd dispersion, as suggested in the recent literature [20–23]. This value also gave a very close fit between the size of Pd particles evaluated from sorption measurement and XRD for 1.20PdN-52 sample (Table 2). This enabled us to adopt this stoichiometry for the other catalysts, too. The dispersion values of Pd deposited on both supports greatly differed depending on the precursor, support and metal loading. $Pd(OAc)_2$ gave distinctly better dispersion on MSA9 at the same Pd loading. On the other hand, the dispersions after deposition of $Pd(NH_3)_4Cl_2{\cdot}H_2O$ were similar on both supports. The largest difference was observed by using $PdCl_2$, i.e. 98% on MSA9 and only 9% on MSA52. Metal dispersion plotted against the overall metal loading is shown in Fig. 3. The dispersion strongly decreased with the deposited Pd amount, which explains the great difference observed for $PdCl_2$ precursor. The decrease in Pd dispersion was pronounced more than the decrease of Pt dispersion on Pt/MSA catalysts prepared by us from a similar MSA50 support [19]. This could be explained by the weaker interaction of the Pd precursors with MSA surface, which could lead to a partial agglomeration of Pd particles during the reduction at the higher temperature. The bimetallic Pd–PtO-9 catalyst showed higher overall metal dispersion in comparison to Pd–PtC-9 and monometallic Pd catalysts of similar metal loadings. We assume that different dispersions of both bimetallic catalysts could be related to the strength of the interaction between both Pt precursors and MSA9. $H_2PtCl_6$ interacts weakly with acidic siliceous supports, which often leads to metal agglomeration during preparation of catalysts [30], while $Pt(NH_3)_4(OH)_2$ is a base adsorbing strongly [31]; this property could preserve a higher Pt dispersion in Pd–PtO-9 as compared to Pd–PtC-9.

Fig. 4 shows TPR pattern of the dried catalysts precursors, normalized to the same weight amount. The pattern of the Pd sample prepared from $Pd(OAc)_2$ show two maxima at 90 °C and 350 °C, ascribed to the reduction of the adsorbed acetate species.

**Table 2**
Composition, CO uptake, metal dispersion, diameter of metal particles and textural properties of catalysts.

| Catalyst | Metal content | | $V_{ads}$ | Dispersion | $D_{metal}$ | $S_{BET}$ | $V_p$ |
|---|---|---|---|---|---|---|---|
| | Pd (%) | Pt (%) | ($ml_{CO}/g_{cat}$) | (%) | (nm) | ($m^2/g$) | ($cm^3/g$) |
| 0.93PdA-52 | 0.93 | 0 | 0.53 | 54 | 2.1 | 340 | 0.39 |
| 1.48PdC-52 | 1.48 | 0 | 0.15 | 9 | 11.7 | 312 | 0.36 |
| 1.20PdN-52 | 1.20 | 0 | 0.34 | 27 | 4.2 (4.15)[a] | 331 | 0.38 |
| 0.92PdA-9 | 0.92 | 0 | 0.85 | 86 | 1.3 | 533 | 0.59 |
| 0.84PdC-9 | 0.84 | 0 | 0.87 | 98 | 1.1 | 550 | 0.59 |
| 1.12PdN-9 | 1.12 | 0 | 0.26 | 22 | 5.0 | 494 | 0.59 |
| 0.41PtO-9 | 0 | 0.41 | 0.24 | 51 | 2.2 | 555 | 0.60 |
| 0.54PtC-9 | 0 | 0.54 | 0.29 | 47 | 2.4 | 522 | 0.59 |
| Pd–PtO-9 | 0.78 | 0.39 | 0.67 | 57 | 2.0 | 564 | 0.60 |
| Pd–PtC-9 | 1.08 | 0.79 | 0.41 | 22 | 5.1 | 564 | 0.62 |

[a] Value in parenthesis determined by X-ray diffraction for Pd(1 1 1) plane.

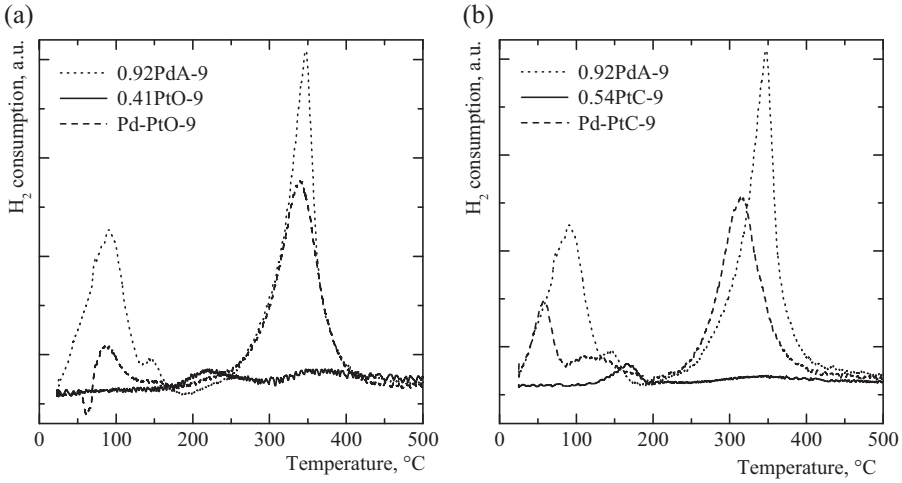


**Fig. 4.** TPR pattern of Pd, Pt and Pd–Pt catalyst precursors. Pd–PtO-9 (a); Pd–PtC-9 (b).

They were absent in the sample prepared from $PdCl_2$ (0.84PdC-9), where only a small $H_2$ consumption at 130 °C was detected (not shown). The Pt catalysts showed small maxima at 170 °C (220 °C) and 300–400 °C, similarly to the already reported values [32]. They were attributed to the reduction of adsorbed $H_2PtCl_6$ and Pt oxide formed by decomposition of $Pt(NH_3)_4(OH)_2$, respectively. The pattern of Pd–PtO-9 and Pd–PtC-9 catalyst precursors show peaks of the acetate species shifted by 7 and 30 °C to the lower reduction temperatures, respectively. The pattern of both bimetallic catalysts were not superpositions of the patterns of their components, confirming that noble metal species interact during reduction with each other. This interaction seems to be stronger in Pd–PtC-9 because of the greater shifts observed in reduction temperatures.

Pd and Pd–Pt catalysts can hold significant amounts of $H_2$, which may play important role in catalytic reactions. $H_2$ is absorbed in the form of β-Pd hydride ($PdH_x$), which decomposition can be monitored by TPD of $H_2$ at around 60–90 °C at atmospheric pressure [33,34]. The TPD patterns of the MSA9-supported catalysts, normalized to the same weight amount, are shown in Fig. 5. The Pt catalysts showed none or a small $H_2$ evolution, classified as chemisorption [35]. The Pd sample (0.92PdA-9) released much more $H_2$ that was desorbed in three temperature regions with maxima at 38 °C (A), around 65 °C (B) and 80 °C (C). In agreement with the literature, they were assigned to desorption from Pd(1 1 1) plane [36], $PdH_x$ decomposition [20,33,34,37] and desorption of strongly adsorbed $H_2$ [38], respectively. It is of interest that the bimetallic Pd–PtO-9 sample showed the most extensive $PdH_x$ decomposition (peak B), while Pd–PtC-9 only negligible one. Table 3 gives the H/Pd ratios calculated for individual desorption peaks by deconvolution of the TPD pattern. The values corresponding to $PdH_x$ decomposition for Pd and Pd–PtO-9 samples were within the range found for the supported Pd catalysts and the solubility limits reported in the literature [33], showing that the Pd particles absorb $H_2$. However, the H/Pd value for Pd–PtC-9 was quite low, the $PdH_x$ formation in this sample was almost completely suppressed. At present, there are no additional experimental data giving information about the extent of alloying of both metals, so the question concerning the presence of the Pd–Pt alloy in both samples remains open. One can speculate that also other factors like Pd:Pt ratio, dispersion of both metals or possibly the effect of residual chlorine in Pd–PtC-9 could influence the interaction of Pd and Pt and their sorption and catalytic properties.

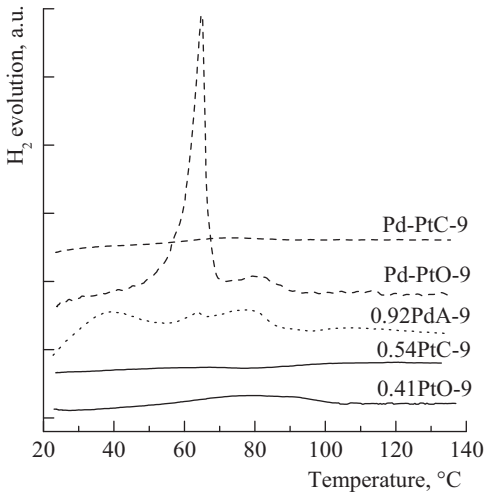


**Fig. 5.** TPD of hydrogen over reduced Pd, Pt and Pd–Pt catalysts.

### 3.3. Activity in HDS of thiophene and benzothiophene

The basic conversion data for HDS of TH, selectivity and the rate constants $k_{TH}$ are summarized in Table 4. The reaction over noble metal catalysts was accompanied by a significant formation of intermediate THT, except for $CoMo/Al_2O_3$ where only $H_2S$ and $C_4$ hydrocarbons were formed. The activity of $CoMo/Al_2O_3$ was stable during several hours on stream, whereas the noble metal catalysts underwent deactivation during the catalytic run. This will be briefly discussed later in Section 3.3.5. The steady state conversion data for BT reaction, selectivity and rate constants $k_{BT}$ are listed in Table 5. Transformation of BT was also accompanied by formation of DHBT, this being again lowest over $CoMo/Al_2O_3$.

**Table 3**
TPD of hydrogen on reduced Pd and Pd–Pt catalysts.

| Catalyst | $V_{des}$ | H/Pd[a] | | | |
|---|---|---|---|---|---|
| | ($ml_{H2}/g_{cat}$) | A | B | C | Total |
| 0.92PdA-9 | 0.22 | 0.10 | 0.02 | 0.12 | 0.24 |
| Pd–PtO-9 | 0.18 | 0.03 | 0.13 | 0.07 | 0.23 |
| Pd–PtC-9 | 0.02 | 0 | 0.02 | 0 | 0.02 |

[a] Letters A, B and C denote the peaks at 38, 65 and 80 °C, respectively.

**Table 4**
Conversion data and thiophene HDS rate constants.

| Catalyst | $W$ (mg) | $x_{TH}$ | $x_{THT}$ | $x_{C4}$ | $x^{o}_{TH}$ | Deact. (%) | $k_{TH}$ ($mol_{TH}$/h $kg_{cat}$) | $k^{o}_{TH}$ ($mol_{TH}$/h $kg_{cat}$) |
|---|---|---|---|---|---|---|---|---|
| 0.93PdA-52 | 20.8 | 0.48 | 0.16 | 0.32 | 0.74 | 35 | 3.7 | 7.4 |
| 1.48PdC-52 | 20.1 | 0.59 | 0.10 | 0.49 | 0.83 | 29 | 5.4 | 10.4 |
| 1.20PdN-52 | 21.2 | 0.60 | 0.13 | 0.47 | 0.78 | 23 | 4.9 | 7.6 |
| 0.92PdA-9 | 9.5 | 0.35 | 0.18 | 0.17 | 0.89 | 61 | 6.2 | 31.0 |
| 0.84PdC-9 | 10.7 | 0.34 | 0.15 | 0.19 | 0.82 | 59 | 5.1 | 20.4 |
| 1.12PdN-9 | 9.6 | 0.38 | 0.17 | 0.20 | 0.79 | 52 | 4.7 | 17.5 |
| 0.41PtO-9 | 8.9 | 0.28 | 0.18 | 0.20 | 0.35 | 20 | 5.1 | 6.6 |
| 0.54PtC-9 | 10.4 | 0.28 | 0.21 | 0.07 | 0.28 | 0 | 4.5 | 4.5 |
| Pd–PtO-9 | 8.4 | 0.68 | 0.09 | 0.44 | 0.82 | 17 | 16.5 | 28.8 |
| Pd–PtC-9 | 8.5 | 0.40 | 0.12 | 0.28 | 0.61 | 34 | 8.4 | 14.4 |
| CoMo | 6.3 | 0.33 | 0.00 | 0.33 | 0.33 | 0 | 6.5 | 6.5 |

Conditions: 280 °C, 2 MPa.

**Table 5**
Conversion data and benzothiophene HDS rate constants.

| Catalyst | $W$ (mg) | $x_{BT}$ | $x_{DHBT}$ | $x_{EB}$ | $k_{BT}$ ($mol_{BT}$/h $kg_{cat}$) |
|---|---|---|---|---|---|
| 0.93PdA-52 | 200 | 0.71 | 0.31 | 0.40 | 48 |
| 1.48PdC-52 | 200 | 0.70 | 0.43 | 0.27 | 47 |
| 1.20PdN-52 | 200 | 0.57 | 0.42 | 0.15 | 32 |
| 0.92PdA-9 | 200 | 0.78 | 0.42 | 0.35 | 58 |
| 0.84PdC-9 | 200 | 0.75 | 0.44 | 0.32 | 54 |
| 1.12PdN-9 | 200 | 0.62 | 0.43 | 0.19 | 38 |
| 0.41PtO-9 | 200 | 0.41 | 0.22 | 0.19 | 20 |
| 0.54PtC-9 | 40 | 0.19 | 0.14 | 0.05 | 41 |
| Pd–PtO-9 | 40 | 0.51 | 0.29 | 0.22 | 138 |
| Pd–PtC-9 | 200 | 0.71 | 0.31 | 0.40 | 48 |
| CoMo | 40 | 0.42 | 0.08 | 0.34 | 107 |

Conditions: 330 °C, 1.6 MPa.

### 3.3.1. Effect of support and Pd precursor

The effect of support and metal precursor on the activity of Pd catalysts in HDS of both model compounds is shown in Fig. 6. The specific activities, expressed per mol of deposited Pd, were substantially higher for the group of catalysts prepared from MSA9. The difference between both supports was most apparent on comparing the initial activities in TH reaction (Fig. 6a). Here the ratios of initial activities of the samples prepared from MSA9 and MSA52 varied between 2 and 4, depending on the kind of Pd precursor. However, as follows from data in Table 4, the Pd catalysts prepared from MSA9 were deactivated faster but this difference diminished after several hours on stream. As far as the effect of Pd precursor is concerned, the catalysts prepared from $Pd(OAc)_2$ and $PdCl_2$ showed usually higher specific activities than those prepared from $Pd(NH_3)_4Cl_2{\cdot}H_2O$ for both model reactions.

### 3.3.2. Effect of metal loading

The effect of metal loading on rate constants $k_{TH}$ is shown in Fig. 7a. The activities of the most catalysts moderately increased to around 2 wt.% of the overall metal content, with the exception of Pd–PtO-9 catalyst which showed much higher activity. A similar situation is shown for BT reaction in Fig. 7b. The $k_{BT}$ values of almost all samples increased to around 1 wt.% Pd and then remained more or less constant, again with the exception of Pd–PtO-9. However, the second bimetallic catalyst (Pd–PtC-9) showed activities close to those for Pd catalysts. Both non-linear dependences suggest the lower utilization of deposited Pd, which is undoubtedly the consequence of decreasing Pd dispersion at the higher metal loadings (Fig. 3). Similar non-linear dependences of the activities of ASA-supported Pd and Pd–Pt catalysts were recently reported for HYD of gas oil [7]. Also in that case, surplus Pd exceeding 1 wt.% loading did not bring any activity improvement. It seems therefore that this is an optimal amount of the active phase, which was easier achieved in Pd–PtO-9 with the overall loading close to 1.2 wt.%.

### 3.3.3. Specific activity and synergetic effect

Fig. 8 shows the relations between specific activities of noble metal catalysts in TH and BT reactions. Fairly good correlation was found between rate constants $k_{TH}$ and $k_{BT}$, with the exception of one Pt catalyst (Fig. 8a). This sample (0.41PtO-9) showed the superior

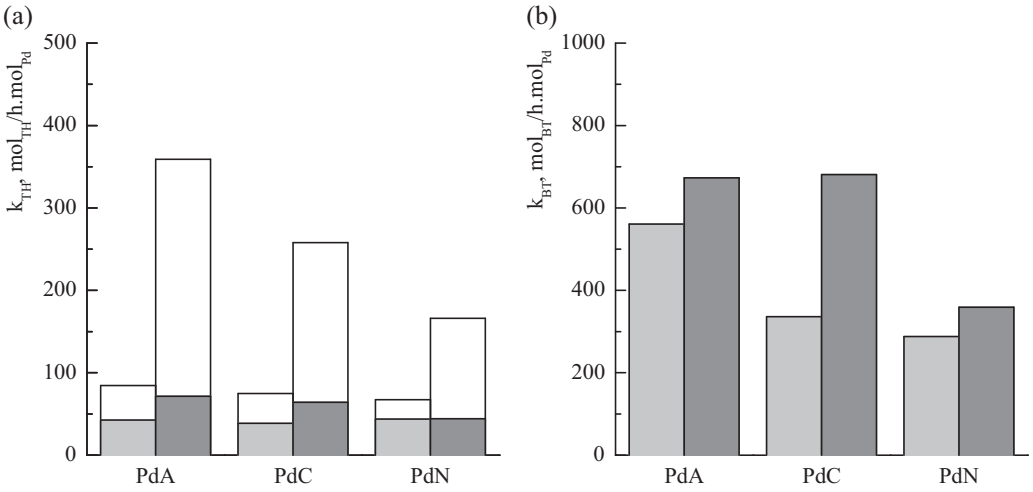


**Fig. 6.** Effect of support and Pd precursor on specific rate constants of overall TH (a) and BT (b) conversion. Initial activity (open bar). Steady state activity (full bar): Pd on MSA52 ▒, Pd on MSA9 ■.

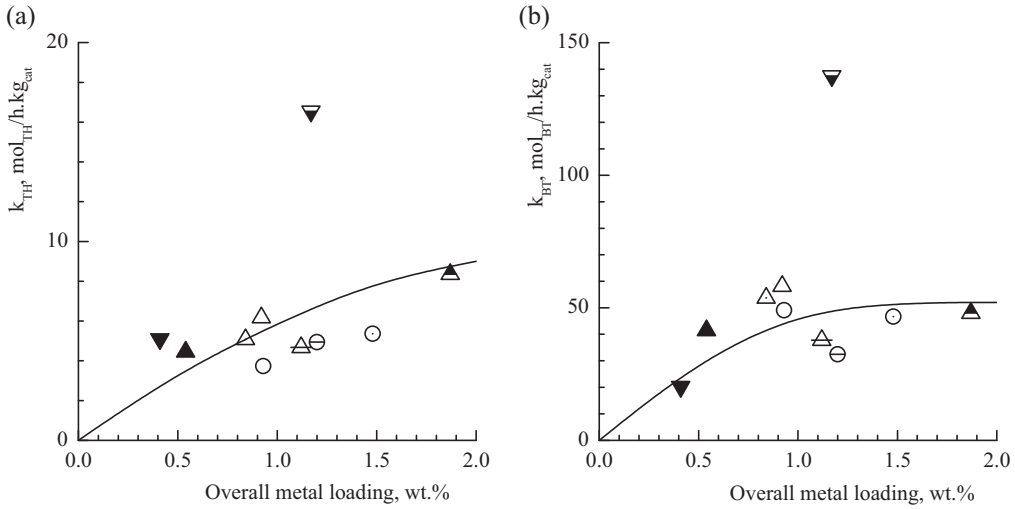


**Fig. 7.** Rate constants of overall conversion of TH (a) and BT (b) as functions of metal loading. 0.93PdA-52 (○), 1.48PdC-52 (⊙), 1.20PdN-52 (⊖), 0.92PdA-9 (△), 0.84PdC-9 (⧋), 1.12PdN-9 (⧋), 0.41PtO-9 (▼), 0.54PtC-9 (▲), Pd–PtO-9 (⧩), Pd–PtC-9 (⧨).

activity in the reaction of TH, but smaller in BT reaction, similarly as the sample prepared from the same Pt precursor and similar MSA11 support in our preceding study [19]. Fig. 8b shows the relation between specific rate constants for formation of sulfur-free products, $C_4$ hydrocarbons (C4) and ethylbenzene (EB). Also in this case, a relation between both activities is apparent. Both Pt catalysts were by far the most efficient among the monometallic catalysts in overall transformations of TH and BT and almost the same holds for the formation of desulfurized products. The higher specific HDS activity of the reduced Pt as compared to Pd is in general agreement with literature data [2,3,5,8,11]. As far as the bimetallic combinations are concerned, one sample showed an excellent HDS efficiency (Pd–PtO-9), well comparable to Pt catalysts, while the other (Pd–PtC-9) was much less active, similarly to Pd catalysts.

Combination of Pd with Pt led to the higher activities observed in different HDS and HYD reactions in many earlier studies [2,3,5–10]. The cause of the high activity or synergetic effect between Pd and Pt has not yet been well understood. It had been ascribed to sulfur tolerance of the active phase on acidic supports [5], the interaction of Pd with Pt [7,39] or to their alloying [8]. In the present work, combination of both metals in Pd–PtO-9 showed significant synergetic effects with the magnitudes of 1.5 and 1.8 for TH and BT transformations, respectively. The values of synergy were close to those observed between ASA-supported Pd and Pt catalysts in HDS of 4-E,6-MDBT [8]. On the other hand, no promotion has occurred over Pd–PtC-9, despite of its overall higher metal content close to 1.9 wt.%. This situation is again similar to that observed already by Reinhoudt et al. [8], where the higher activity had been achieved with the Pd:Pt = 4 ratio at the lower metal loading. In our case, the Pd:Pt ratio in the more active Pd–PtO-9 was 3.7, i.e. more favorable for optimum performance. Both bimetallic catalysts differed in several points. Different Pt precursors affected the overall metal dispersion, the extent of interaction of the Pd and Pt species and also the amounts of $H_2$ absorbed in the $PdH_x$ phase. It is interesting that the Pd–PtC-9 sample showed a very small $H_2$ absorption and only poor activity, in contrast to most active Pd–PtO-9 with high content of the $PdH_x$ phase. This result suggests, that $H_2$ present in this form could positively influence the rate of HDS and then, the observed synergy in Pd–PtO-9 could most likely be ascribed to the interaction between Pt and Pd particles. It is well documented that $PdH_x$ phase with the composition approaching to H/Pd = 0.3 also exists at 280 °C and 2 MPa of $H_2$ [40]. Thus, it is possible that some fraction of Pd plays a role as $H_2$ storage medium also under

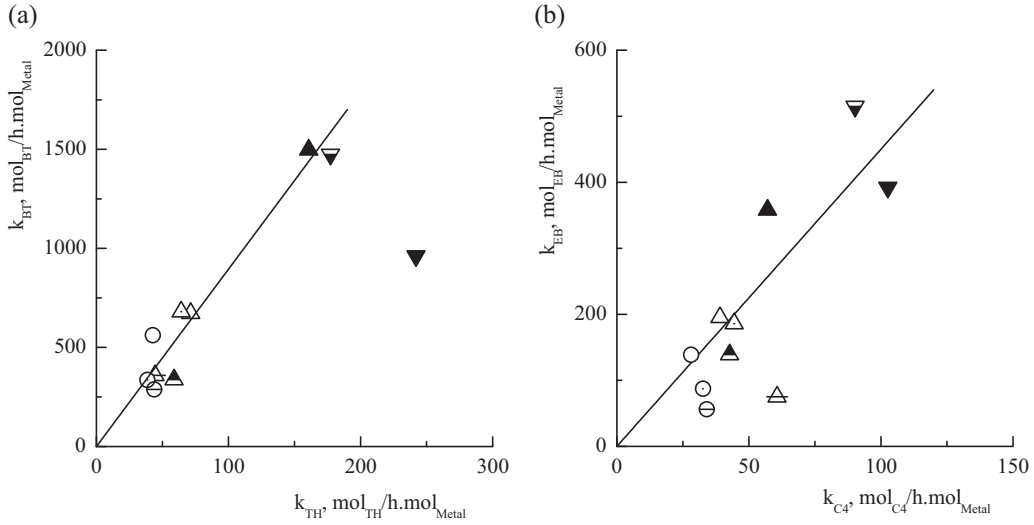


**Fig. 8.** Relation between specific rate constants for reactions of BT and TH. Overall transformation (a). Desulfurized products (b). Symbols same as in Fig. 7.

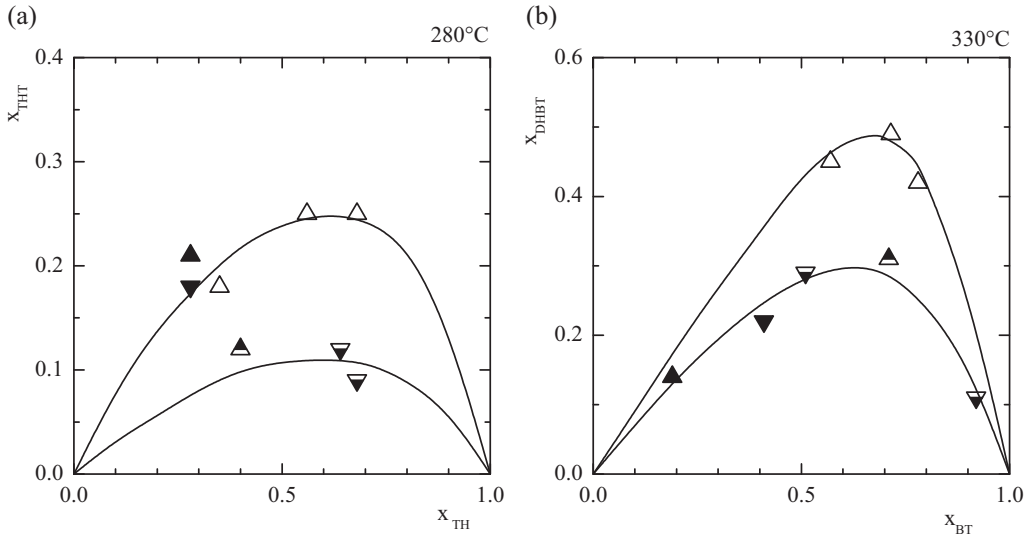


**Fig. 9.** Conversions in THT (a) and DHBT (b) as functions of overall TH and BT conversions. Symbols same as in Fig. 7.

conditions of HDS reaction, in co-operation with the dispersed Pt activating $H_2$. However, this idea does not rule out additional possible effects of the support acidity on sulfur tolerance of the active phase or alloying. The results obtained in the present work show that a proper substitution of minor part of Pd for Pt leads to the great activity improvement approaching the highest activity level attainable with Pt catalysts (Fig. 8). This is desirable from the point of view of the catalyst price, since Pd is substantially cheaper than Pt.

### 3.3.4. Selectivity in THT and DHBT formation

Reduced noble metals generally possess an excellent HYD activity, which leads to the formation of considerable amounts of hydrogenated reaction intermediates in HDS, preferentially when deposited on acidic supports like ASA and zeolites. ASA- and NaHY-supported Pd sulfide [41] and reduced Pt on zeolites or oxide supports [42] showed high selectivity in THT formation at 2 MPa and at 240 and 300 °C, respectively, i.e. under conditions similar to ours. Also in the present work, both HDS reactions over noble metals were accompanied by formation of THT and DHBT. Fig. 9 shows the extent of their formation as functions of the overall conversions $x_{TH}$ ($x_{BT}$). The monometallic Pd and Pt catalysts gave in HDS of TH higher amounts of THT than both bimetallic Pd–Pt catalysts and similar situation seems to hold for BT reaction. However, the 0.41PtO-9 catalyst showed the same selectivity in DHBT formation as the bimetallic catalysts. These results agree with the more extensive formation of partly hydrogenated intermediates over Pd/ASA compared to Pd–Pt/ASA in HDS of DBT [9] and 4,6-DMDBT [10]. All these data suggest that the Pd–Pt catalysts possess higher C–S bond hydrogenolytic activity than monometallic Pd catalysts for both simple and more complicated sulfur-containing molecules.

### 3.3.5. Comparison with conventional catalyst

The activity data for HDS of TH over all the catalysts studied are summarized in Table 4. Almost all noble metal catalysts were deactivated during the catalytic run, in contrast to the stable activity of the conventional catalyst. This activity decay was most significant for Pd catalysts, especially for those prepared from MSA9. This could be ascribed to its higher acidity, leading to more extensive coking. It was shown that the strength of the acidic sites of a similar kind of Pd/Al-MCM-41 catalysts played important role in deactivation of these catalysts in HDS of TH [12]. On the other hand, the Pd–Pt catalysts were deactivated much less than Pd ones. This agrees with much smaller or no deactivation of Pd–Pt/USY in HDS of thiophene [3] and Pd–Pt/ASA in HDS of DBT [9] in comparison to their Pd counterparts. In those studies, the higher HYD activity and sulfur tolerance of the mixed phase were proposed to explain this behavior. The metallic sites of Pd and Pd–Pt catalysts are obviously most active and partial sulfidation during HDS can reduce their activity. We assume that lower sulfur tolerance of our Pd catalysts could be additional reason for their faster deactivation. Table 4 shows that the MSA-supported Pd catalysts exhibited fairly high initial activities in TH reaction, which exceeded the activity of $CoMo/Al_2O_3$. However, the activities gradually decreased after several hours below that of $CoMo/Al_2O_3$ due to the strong deactivation. Both bimetallic Pd–Pt samples remained more active than $CoMo/Al_2O_3$ also in the steady state due to their higher activity levels and smaller deactivation. Similarly to TH reaction, Pd–PtO-9 was also the most active in BT reaction (Table 5). The order of the catalyst activities found in the present work, i.e. Pd–Pt > CoMo > Pd follows activity trends observed in TH and BT reactions earlier [2,3].

## 4. Conclusions

Post-synthesis leaching of the mesoporous silica–alumina containing 52 wt.% $Al_2O_3$ with nitric acid led to samples with the lower $Al_2O_3$ content of 9 wt.%, stronger Brønsted acidity and higher surface area. The leaching mostly removed the non-acidic form of $Al_{oct}$ species and exposed the fraction of $Al_{tet}$ species. The higher acidity and surface area of the modified support greatly improved the activity of Pd catalysts in HDS of thiophene. $Pd(OAc)_2$ as a precursor gave the most active catalyst per mol of Pd. However, the specific activities of Pd catalysts in HDS of thiophene and benzothiophene were lower than those attained with Pt catalysts. The bimetallic Pd–Pt catalyst prepared by co-impregnation of the more acidic MSA with $Pd(OAc)_2 + Pt(NH_3)_4(OH)_2$ was most active in HDS of thiophene and benzothiophene. In this case, we propose that interaction of Pt and Pd obviously led to high content of activated hydrogen in the Pd phase, which most likely contributed to the high HDS activity. Leaching of the part of $Al_2O_3$ phase from MSA significantly improved HDS activities of the Pd catalysts similarly to the same effect observed previously by us for Pt catalysts. MSA modified in this way seems to be a promising support of noble metal catalysts and thus an alternative to other mesoporous siliceous materials.

## Acknowledgement

The financial support of the Czech Science Foundation (grants 104/09/0751 and P106/11/0902) is gratefully acknowledged.

## References

[1] S.D. Lin, Ch. Song, Catal. Today 31 (1996) 93–104.
[2] W. Qian, Y. Yoda, Y. Hirai, A. Ishihara, T. Kabe, Appl. Catal. A 184 (1999) 81–88.
[3] M. Sugioka, F. Sado, Y. Matsumoto, N. Maesaki, Catal. Today 29 (1996) 255–259.
[4] H. Yasuda, Y. Yoshimura, Catal. Lett. 46 (1997) 43–48.
[5] Y. Yoshimura, M. Toba, T. Matsui, M. Harada, Y. Ichihashi, K.K. Bando, H. Yasuda, H. Ishihara, Y. Morita, T. Kameoka, Appl. Catal. A 322 (2007) 152–171.
[6] R.M. Navarro, B. Pawelec, J.M. Trejo, R. Mariscal, J.L.G. Fierro, J. Catal. 189 (2000) 184–194.
[7] T. Fujikawa, K. Idei, T. Ebihara, H. Mizuguchi, K. Usui, Appl. Catal. A 192 (2000) 253–261.
[8] H.R. Reinhoudt, R. Troost, A.D. van Langeveld, J.A.R. van Veen, S.T. Sie, J.A. Moulijn, in: B. Delmon, G.F. Froment, P. Grange (Eds.), Hydrotreatment and Hydrocracking of Oil Fractions, Elsevier Science, 1999.
[9] V.L. Barrio, P.L. Arias, J.F. Cambra, M.B. Güemez, B. Pawelec, J.L.G. Fierro, Catal. Commun. 5 (2004) 173–178.
[10] A. Niquille-Rothlisberger, R. Prins, Catal. Today 123 (2007) 198–207.
[11] Y. Kanda, T. Aizawa, T. Kobayashi, Y. Uemichi, S. Namba, M. Sugioka, Appl. Catal. B 77 (2007) 117–124.
[12] A.M. Venezia, R. Murania, V. La Parola, B. Pawelec, J.L.G. Fierro, Appl. Catal. A 383 (2010) 211–216.
[13] F. Zhou, X. Li, A. Wang, L. Wang, X. Yang, Y. Hu, Catal. Today 150 (2010) 218–223.
[14] A. Gola, B. Rebours, E. Milazzo, J. Lynch, E. Benazzi, S. Lacombe, L. Delevoye, C. Fernandes, Microporous Mesoporous Mater. 40 (2000) 73–83.
[15] X. Li, A. Wang, Y. Wang, Y. Chen, Y. Liu, Y. Hu, Catal. Lett. 84 (2002) 107–113.
[16] Z. Vít, O. Šolcová, Microporous Mesoporous Mater. 96 (2006) 197–204.
[17] D. Gulková, Z. Vít, Stud. Surf. Sci. Catal. 162 (2006) 489–496.
[18] D. Gulková, Y. Yoshimura, Z. Vít, Appl. Catal. B 87 (2009) 171–180.
[19] Z. Vít, D. Gulková, L. Kaluža, S. Bakardieva, M. Boaro, Appl. Catal. B 100 (2010) 463–471.
[20] F. Pinna, M. Signoretto, G. Strukul, S. Polizzi, N. Pernicone, React. Kinet. Catal. Lett. 60 (1997) 9–13.
[21] A. Guerrero-Ruiz, S. Yang, Q. Xin, A. Maroto-Valiente, M. Benito-Gonzalez, I. Rodriguez-Ramos, Langmuir 16 (2000) 8100–8106.
[22] F. Pinna, F. Menegazzo, M. Signoretto, P. Canton, G. Fagherazzi, N. Pernicone, Appl. Catal. A 219 (2001) 195–200.
[23] P. Canton, G. Fagherazzi, M. Battagliarin, F. Menegazzo, F. Pinna, N. Pernicone, Langmuir 18 (2002) 6530–6535.
[24] J.R. Anderson, K.C. Pratt, Introduction to Characterization and Testing of Catalysts, Academic Press (Harcourt Brace Jovanovish Publishers), New York, 1985, p. 64.
[25] F.M. Bautista, J.M. Campelo, A. Garcia, D. Luna, J.M. Marinas, A.A. Romero, Catal. Lett. 24 (1994) 293–301.
[26] Z. Vít, D. Gulková, L. Kaluža, M. Zdražil, J. Catal. 232 (2005) 447–455.
[27] T. Klicpera, M. Zdražil, J. Catal. 206 (2002) 314–320.
[28] G. Crépeau, V. Montouillout, A. Vimont, L. Mariey, T. Cseri, F. Maugé, J. Phys. Chem. B 110 (2006) 15172–15185.
[29] E.J.M. Hensen, D.G. Poduval, P.C.M.M. Magusin, A.E. Coumans, J.A.R. van Veen, J. Catal. 269 (2010) 201–218.
[30] J.T. Miller, M. Schreier, A.J. Kropf, J.R. Regalbuto, J. Catal. 225 (2004) 203–212.
[31] A. Goguet, M. Aouine, F.J.C.S. Aires, A. De Mallmann, D. Schweich, J.P. Candy, J. Catal. 209 (2002) 135–144.
[32] V.G. Baldovino-Medrano, P. Eloy, E.M. Gaigneaux, S.A. Giraldo, A. Centeno, J. Catal. 267 (2009) 129–139.
[33] M. Bonarowska, J. Pielaszek, W. Juszcyk, Z. Karpinski, J. Catal. 195 (2000) 304–315.
[34] M. Bonarowska, Z. Karpinski, Catal. Today 137 (2008) 498–503.
[35] R. Giannantonio, V. Ragaini, P. Magni, J. Catal. 146 (1994) 103–115.
[36] G.E. Gdowski, T.E. Felter, R.H. Stulen, Surf. Sci. Lett. 181 (1987) L147–L155.
[37] N.K. Nag, J. Phys. Chem. B 105 (2001) 5945–5949.
[38] V. Ragaini, R. Giannantonio, P. Magni, L. Lucarelli, G. Leofanti, J. Catal. 146 (1994) 116–125.
[39] T. Fujikawa, K. Tsuji, H. Mizuguchi, H. Godo, K. Idei, K. Usui, Catal. Lett. 63 (1999) 27–33.
[40] J.M. Joubert, S. Thiébaut, J. Nucl. Mater. 395 (2009) 79–88.
[41] A.V. Maskhina, L.G. Sakhaltueva, Petrol. Chem. 42 (2002) 335–340.
[42] Z.R. Ismagilov, S.A. Yashnik, A.N. Startsev, A.I. Boronin, A.I. Stadnichenko, V.V. Kriventsov, S. Kasztelan, D. Guillaume, M. Makkee, J.A. Moulijn, Catal. Today 144 (2009) 235–250.